

SUPPLEMENTARY MATERIALS

Massarilactones D and H, phytotoxins produced by *Kalmusia variispora*, associated with grapevine trunk diseases (GTDs) in Iran

Alessio Cimmino^{a,*}, Zeinab Bahmani^b, Marco Masi^a, Roberta Di Lecce^a, Jahanshir Amini^b, Jafar Abdollahzadeh^{b,*}, Angela Tuzi^a and Antonio Evidente^a

^aDipartimento di Scienze Chimiche, Università di Napoli Federico II, Complesso Universitario Monte S. Angelo, Via Cintia 4, 80126 Napoli, Italy; alessio.cimmino@unina.it (A.C), marco.masi@unina.it (M.M.), roberta.dilecce@unina.it (R.D.L.), angela.tuzi@unina.it (A.T.), evidente@unina.it (A.E.)

^bDepartment of Plant Protection, Agriculture Faculty, University of Kurdistan, P.O. Box 416, Sanandaj, Iran; z_bahmani65@yahoo.com (Z.B.), jamini@uok.ac.ir (J.A.), j.abdollahzadeh@uok.ac.ir (J.A.)

ABSTRACT: A strain of *Kalmusia variispora* associated with grapevine trunk diseases (GTDs) was identified in Iran and induced disease symptoms on the host in greenhouse conditions. The grapevine pathogens are able to produce a plethora of toxic metabolites belonging to different classes of naturally occurring compounds. Two homogeneous compounds were isolated from the organic extract of *K. variispora* culture filtrates. They were identified by physic (specific optical rotation), and spectroscopic (essentially 1D and 2D ¹H and ¹³C NMR and HR ESIMS) methods as the fungal polyketides massarilactones D and H (**1** and **2**). The unassigned absolute configuration of massarilactone D was unambiguously determined by X-ray diffractometric analysis. Massarilactones D and H showed phytotoxic activity on *Vitis vinifera* L. at both concentrations used and depending from the days of inoculation. Phytotoxicity is also increased when the *O,O',O''*-triacyl derivative of massarilactone D (**3**) was assayed on the host plant. This is the first report on the investigation of phytotoxic metabolites produced by *K. variispora* isolated from infected grapevine in Iran and they seem to be involved in the development of disease symptoms.

KEYWORDS: Grapevine trunk diseases (GTDs), *Kalmusia variispora*, phytotoxins, massarilactones D and H, absolute configuration of massarilactone D

1. General experimental procedures

Optical rotations were measured in a MeOH solution on a Jasco P-1010 digital polarimeter (Tokyo, Japan); ^1H NMR spectra were recorded at 400 or 500 and 100 or 125 MHz in CD_3OD , Acetone- D_6 or otherwise noted, on Bruker (Karlsruhe, Germany) and Varian (Palo Alto, CA, USA) instruments. The same solvents were also used as an internal standard. ESI MS and LC/MS analyses were performed using the LC/MS TOF system AGILENT (Agilent Technologies, Milan, Italy) 6230B, HPLC 1260 Infinity. Analytical and preparative TLCs were carried out on silica gel (Kieselgel 60, F254, 0.25 and 0.5mm respectively) or on reverse phase (RP-18 F254, 0.25 mm) plates (Merck, Darmstadt, Germany). The spots were visualized by exposure to UV radiation, or by spraying first with 10% H_2SO_4 in MeOH, and then with 5% phosphomolybdic acid in EtOH, followed by heating at 110 C for 10 min. Column chromatography was performed using silica gel (Kieselgel 60, 0.063-0.200 mm) (Merck).

2. Identification of the fungal metabolites

Massarilactone D (**1**): white crystals; $[\alpha]_{\text{D}}^{25}$ -94.0 (*c* 0.2) [lit. Kock et al. 2007: $[\alpha]_{\text{D}}^{20}$ -116.1 (*c* = 0.56, MeOH) ^1H NMR data see Table S1. These data are in agreement with those previously reported (Kock et al. 2007); ESIMS (+) m/z 507 $[2\text{M} + \text{Na}]^+$, 265.0797 (calcd. 265.0688 for $\text{C}_{11}\text{H}_{14}\text{NaO}_6$ $[\text{M} + \text{Na}]^+$).

Massarilactone H (**2**): amorphous; $[\alpha]_{\text{D}}^{25}$ -74.0 (*c* 0.4) [lit. Zhang et al. 2012: $[\alpha]_{\text{D}}^{25}$ -73.9 (*c* 0.23, MeOH) ^1H NMR data are in agreement with those previously reported (Zhang et al. 2012); ESIMS (+) m/z 471 $[2\text{M} + \text{Na}]^+$, 247.0591 (calcd. 247.0582 for $\text{C}_{11}\text{H}_{12}\text{NaO}_5$ $[\text{M} + \text{Na}]^+$).

3. 3,4,7-O,O',O''-Acetyl of massarilactone D (3). Massarilactone D (**2**, 7.5 mg), dissolved in pyridine (50 μL), was converted in its corresponding triacetyl ester (**3**) by acetylation with Ac_2O (50 μL). The reaction was carried out under stirring overnight at room temperature. It was stopped with MeOH, and the azeotrope formed by addition of C_6H_6 was evaporated under nitrogen stream. The residue was then purified by TLC eluted with $\text{CHCl}_3/i\text{-PrOH}$ (95/5, v/v) yielded **4** as a homogeneous compound (6.9 mg). Derivative **4** had: ^1H NMR data see Table S1; ESIMS m/z 759 $[2\text{M} + \text{Na}]^+$, 391 $[\text{M} + \text{Na}]^+$, 309 $[\text{M} + \text{H} - \text{AcOH}]^+$, 249 $[\text{M} + \text{H} - 2\text{x AcOH}]^+$, 207 $[\text{M} + \text{H} - 2\text{xAcOH} - \text{CH}_2\text{CO}]^+$.

4. X-ray crystallographic analysis of massarilactone D

Single crystals of massarilactone D (**1**) suitable for X-ray structure analysis were obtained by slow evaporation from *i*-PrOH solution at room temperature. One selected crystal of **1** was mounted in flowing N₂ at 173 K on a Bruker-Nonius KappaCCD diffractometer equipped with Oxford Cryostream apparatus (graphite monochromated MoK α radiation $\lambda = 0.71073$ Å, CCD rotation images, thick slices, φ and ω scans to fill the asymmetric unit). A semiempirical absorption correction (multiscan, SADABS) was applied. The structure was solved by direct methods using the SIR97 program (Altomare et al., 1999) and anisotropically refined by the full matrix least-squares method on F² against all independent measured reflections using the SHELXL-2018/3 (Sheldrick, Acta Cryst., 2015) and WinGX software (Farrugia et al., 2012). One solvent water molecule was found in the asymmetric unit. All the hydroxy H atoms and the water H atoms were individuated in difference Fourier maps and freely refined with Uiso(H) equal to 1.2Ueq of the carrier atom. All the other H atoms were placed in calculated positions and refined accordingly to a riding model with C–H distances in the range 0.95–1.00 Å and Uiso(H) equal to 1.2Ueq of the carrier atom (1.5Ueq for Cmethyl). The 2*S*,3*R*,4*S*,7*S* absolute configuration at C2,C3,C4,C7 was determined by performing X-ray diffraction data collection according to the literature methods reported to assign the absolute configuration in light-atom structures when MoK α radiation is used. The calculated absolute parameters and the Bayesian statistics P values indicate a very probability that the absolute configuration is correctly assigned (Escudero-Adan et al., 2014; Parsons et al., 2013; Parsons, 2017).

Crystallographic Data of **1**. C₁₁H₁₄O₆·H₂O, M =260.24, orthorhombic, P212121, a = 5.6990(11)Å, b = 8.2310(9)Å, c = 25.876(4) Å, $\alpha = \beta = \gamma = 90^\circ$, V = 1213.8(3)Å³, T = 173(2) K, Z = 4, Dcalcd = 1.424 Mg/m³, crystal size 0.50 × 0.18 × 0.08 mm³, F(000) = 552, absorption coefficient 0.120 mm⁻¹, reflections collected 33095, independent reflections 3405 [Rint = 0.0376], final R indices [I > 2 σ (I)] R1 = 0.0332, wR2 = 0.0861, R indices (all data) R1 = 0.0413, wR2 = 0.0861. Absolute parameters: Flack x determined using 1143 quotients: 0.03(19); Parsons z: -0.04(19); Bayesian statistics: P2(true) = 1.00, P3(true) = 0.992, P3(rac-twin) = 0.008, P3(false) = 0.3.10⁻⁹, Hooft y = 0.06(14), Bijvoet Pairs 1345, Friedel coverage 92%. Absolute structure parameters were calculated using the programs SHELXL-2018/3 and PLATON-v30118. The figures were generated using ORTEP-3 (Farrugia et al., 2012) and Mercury CSD 4.0 (Macrae et al., 2008).

The crystallographic data for massarilactone D (**1**) has been deposited in the Cambridge Crystallographic Data Centre with deposition numbers CCDC 2006859. These data can be obtained free of charge from the Cambridge Crystallographic Data Centre via www.ccdc.cam.ac.uk/.

5. Phytotoxic bioassay

Massarilactone D and H and the 3,4,7-*O,O',O''*-triacyetyl derivative of massarilactone D (**1**, **2** and **3**) were assayed under the same conditions as previously reported (Reveglia et al. 2019) The compounds were dissolved in 40 μL of MeOH, and the volume was adjusted to 1 mL in sterile distilled water (SDW). The bioassays were conducted at 1×10^{-3} and 1×10^{-4} M. Disease-free grapevine leaves were harvested from the fifth node of glasshouse grown *Vitis vinifera* L., and the petiole of each leaf was immersed in a vial containing 1 mL of each the solutions for 24 h. SDW with 4% MeOH was used as the negative control. The leaves were then transferred to a new vial with 2 mL of SDW, placed in a growth chamber with a 12 h light/12 h darkness period at 28 °C, and maintained for an additional 28 h period. Lesions on the leaf surface were visually recorded after 48 h. Each experiment was conducted in triplicate.

6. References

- Altomare A, Burla MC, Camalli M, Cascarano GL, Giacobazzo C, Guagliardi A, Moliterni AGG, Polidori G, Spagna R. 1999. SIR97: a new tool for crystal structure determination and refinement. *J Appl Cryst.* 32:115-119.
- Escudero-Adan, EC, Benet-Buchholz J, Ballester P. 2014. The use of Mo $K\alpha$ radiation in the assignment of the absolute configuration of light-atom molecules; the importance of high-resolution data. *Acta Cryst.* B70:660-668.
- Farrugia LJ. 2012. WinGX and ORTEP for Windows: an update. *J Appl Cryst.* 45:849-854.
- Macrae CF, Bruno IJ, Chisholm JA, Edgington PR, McCabe P, Pidcock E, Rodriguez-Monge L, Taylor R, van de Streek J, Wood PA. 2008. Mercury CSD 2.0—new features for the
- Parsons, S 2017. Determination of absolute configuration using X-ray diffraction. *Tetrahedron: Asymmetry.* 28:1304-1313.
- Parsons S, Flack HD, Wagner T. 2013. Use of intensity quotients and differences in absolute structure refinement. *Acta Cryst.* B69:249-259.
- Reveglia P, Savocchia S, Billones-Baaijens R, Masi M, Cimmino A, Evidente A. 2019. Phytotoxic metabolites by nine species of Botryosphaeriaceae involved in grapevine dieback in Australia and identification of those produced by *Diplodia mutila*, *Diplodia seriata*, *Neofusicoccum australe* and *Neofusicoccum luteum*. *Nat Prod Res.* 33:2223-2229.
- Sheldrick GM. 2015. Crystal structure refinement with SHELXL. *Acta Cryst.* C71:3-8.

Table S1. NMR Data of Massarilactone D and its 3,4,7-*O,O'*; *O''*-Triacetyl-Derivative (**1** and **3**)

	1 ^a	3
N.	δ_{H} (<i>J</i> in Hz)	δ_{H} (<i>J</i> in Hz)
2	4.85 dd (7.9, 4.2)	5.01 br d (7.9)
3	3.83 t (4.2)	4.69 br s
4	4.31 d (4.2)	5.17 br s
8	5.79 ddd (15.0, 7.9, 1.5)	5.71 br dd (15.0, 7.9)
9	5.95 dq (15.0, 6.3)	5.94 br dq (15.0, 6.7)
Me-10	1.77 dd (6.3, 1.5)	1.77 br s ^b
Me-11	1.63 s	1.77 br s ^b
MeCO		2.1 br s ^c

^aThese values are very similar to those previously reported by Kock et al. 2007, which were recorded in CD₃OD

^{b, c}These signal integrating for 6 and 9 H, respectively, are overlapped signals

Table S2. Crystal data and structure refinement for massarilactone D (**1**).

Empirical formula	C ₁₁ H ₁₆ O ₇
Formula weight	260.24
Temperature	173(2) K
Wavelength	0.71073 Å
Crystal system	Orthorhombic,
space group	P 2 ₁ 2 ₁ 2 ₁
Unit cell dimensions	a = 5.6990(11) Å α = 90° b = 8.2310(9) Å β = 90° c = 25.876(4) Å γ = 90°
Volume	1213.8(3) Å ³
Z	4
Calculated density	1.424 Mg/m ³
Absorption coefficient	0.120 mm ⁻¹
F(000)	552
Crystal size	0.500 x 0.180 x 0.080 mm
Theta range for data collection	2.597° to 30.032°
Limiting indices	-7 ≤ h ≤ 7, -11 ≤ k ≤ 11, -36 ≤ l ≤ 36
Reflections collected / unique	33102 / 3406 [R(int) = 0.0376]
Refinement method	Full-matrix least-squares on F ²
Data / restraints / parameters	3405 / 0 / 181
Goodness-of-fit on F ²	1.079
Final R indices [I > 2σ(I)]	R1 = 0.0332, wR2 = 0.0815
R indices (all data)	R1 = 0.0413, wR2 = 0.0861
Absolute structure parameter	0.03(19)
Extinction coefficient	n/a
Largest diff. peak and hole	0.302 and -0.259 e.Å ⁻³

Table S3. Selected bond lengths [Å] for massarilactone D (**1**).

C(3)-O(9)	1.428(2)
C(4)-O(8)	1.427(2)
C(4A)-C(7A)	1.337(2)
C(4A)-C(5)	1.447(2)
C(5)-O(7)	1.213(2)
C(7)-O(10)	1.378(2)

Table S4. Hydrogen bonds for massarilactone D (**1**) [Å and °].

D-H...A	d(D-H)	d(H...A)	d(D...A)	<(DHA)
O(10)-H(10)...O(8)# 1	0.84(3)	1.90(3)	2.7254(19)	165(2)
O(9)-H(9A)...O(7)#2	0.88(3)	1.94(2)	2.8037(18)	169(2)
O(8)-H(8A)...O(11)#3	0.77(3)	2.04(3)	2.759(2)	154(3)
O(11)-H(11D)...O(7)#2	0.96(3)	2.35(3)	3.004(2)	125(2)
O(11)-H(11E)...O(9)#4	1.00(3)	1.84(3)	2.821(2)	163(3)

Symmetry transformations used to generate equivalent atoms:

#1 $x+1, y, z$ #2 $-x+1, y+1/2, -z+3/2$ #3 $x-1, y, z$ #4 $-x+2, y-1/2, -z+3/2$

Table S5. Level of phytotoxic activity of massarilactones D and H and 3,4,7-*O,O',O''*-triacetyl-massarilactone D (**1-3**)

Compound	Level of toxicity ^a			
	24 h post inoculation		72 h post inoculation	
	Concentration (M)		Concentration (M)	
	10 ⁻³	10 ⁻⁴	10 ⁻³	10 ⁻⁴
Massarilactone D (1)	1	1	3	2
Massarilactone H (2)	1	1	3	3
3,4,7- <i>O,O',O''</i> -Triacetyl-massarilactone D (3)	3	2	4	4
Negative control ^b	0	0	0	0

^aSeverity scale: (0) no symptoms; (1) slight wilting; (2) moderate wilting; (3) necrotic spots; (3) severe necrosis and shriveling. The experiment were performed in triplicate.

^b4% MeOH in bidistilled water



Figure S1. A) Grapevine (*Vitis vinifera* L.) trunk with vascular discoloration and necrosis of wood induced by *Kalmusia variispora*; B) Vascular discoloration and necrosis induced of *K. variispora* in greenhouse on 2 years hold.

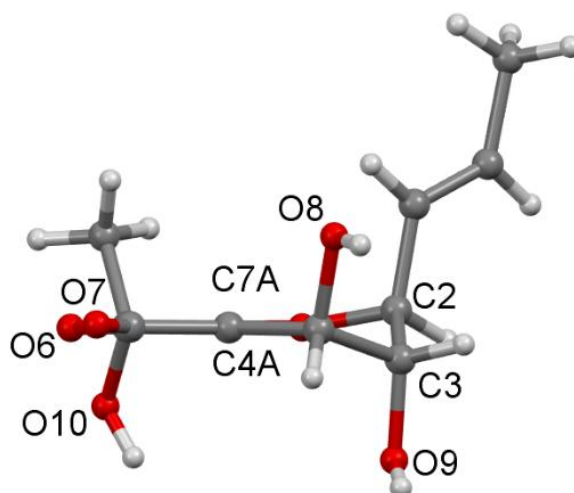


Figure S2. Massarilactone D (**1**) viewed along C4A-C7A bond direction (Ball-and-stick style).

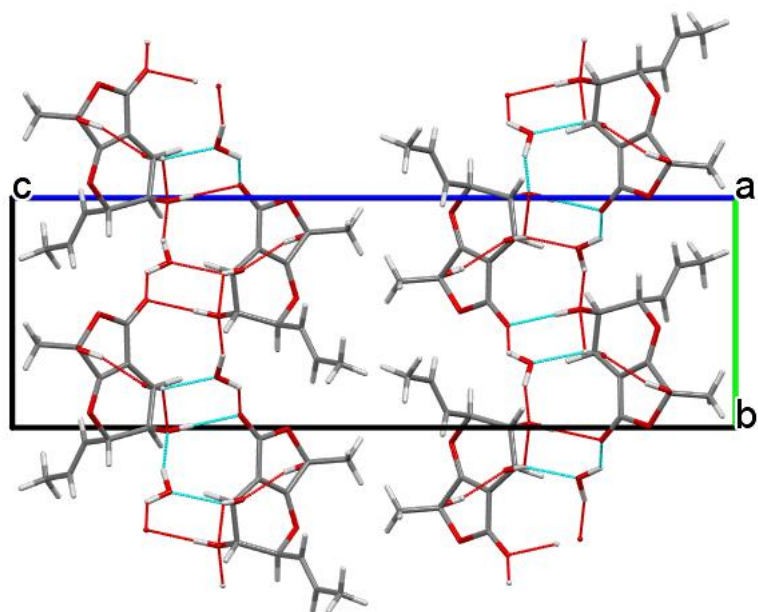


Figure S3. Crystal packing of massarilactone D (**1**) viewed down **a** axis (Capped-stick style). The hydrogen bonding pattern involving solvent water molecules is shown as dashed cyan and red lines.

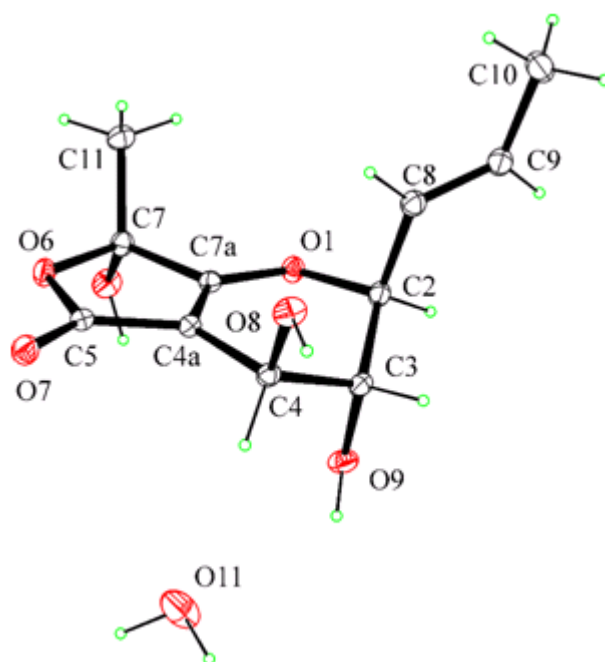


Figure S4. Ortep view of Massarilactone D (**1**) and crystallization water molecule with atoms labels. Thermal ellipsoids are drawn at 30% probability level.



Figure S5. Symptoms caused by compounds **1–3** on leaves of *Vitis vinifera* L. in vitro at concentration of 10^{-4} M at 72 h post inoculation. Control: 4% MeOH in bidistilled water.

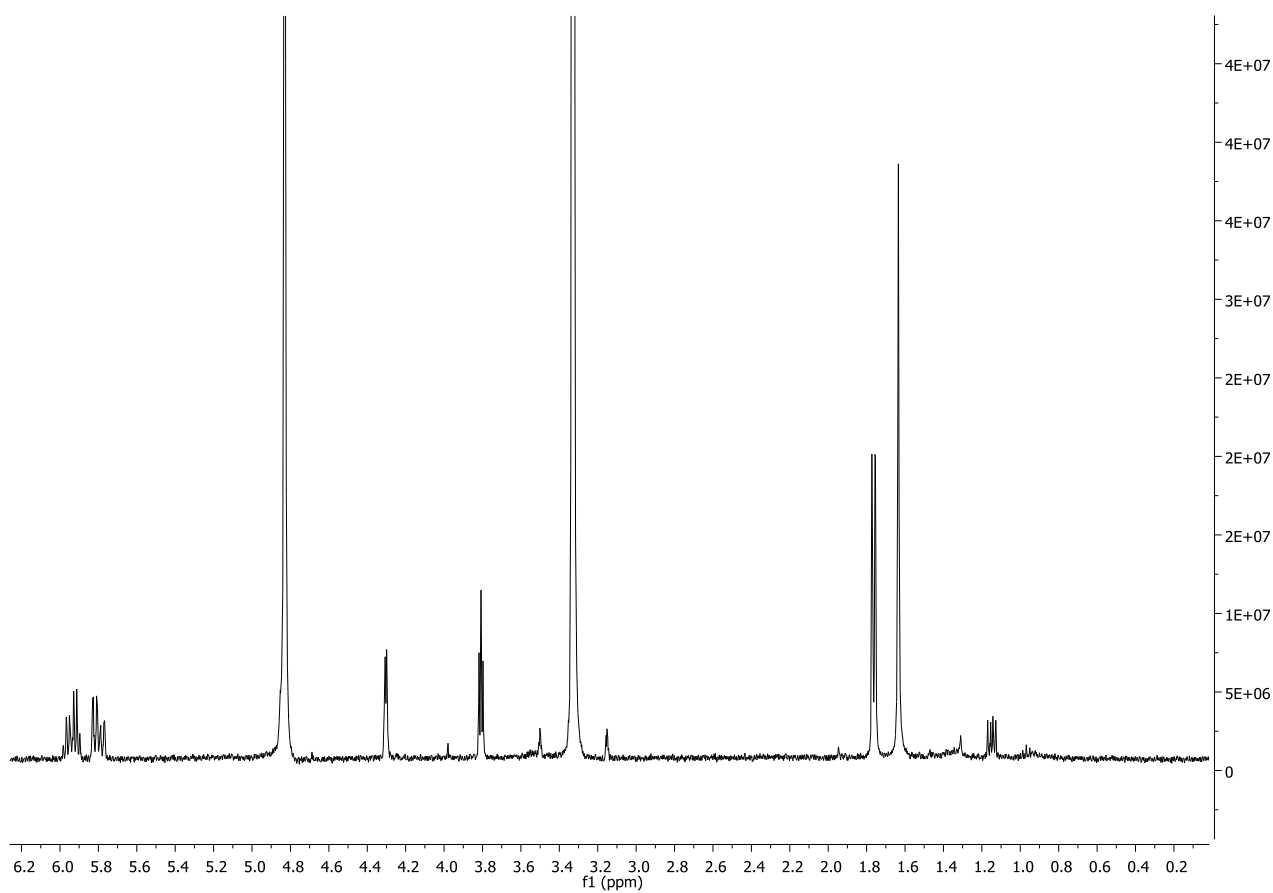


Figure S6. ^1H NMR of massarilactone D (**1**) recorded in CD_3OD at 400 MHz.

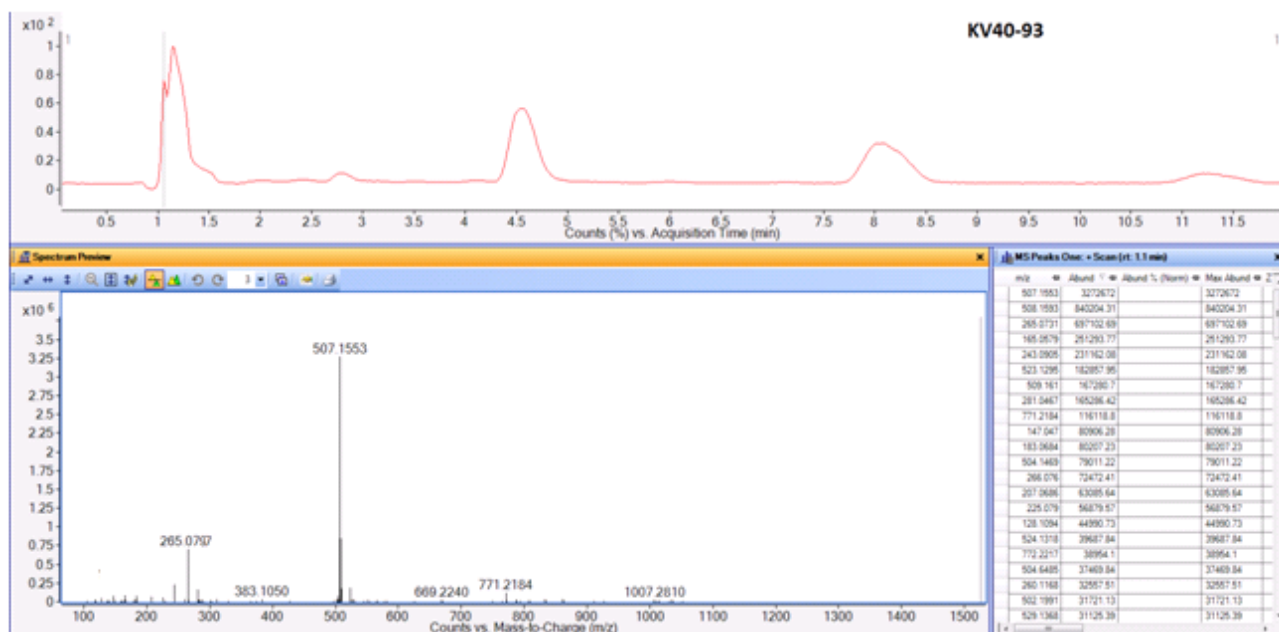


Figure S7. HR ESI MS of massarilactone D (**1**), recorded in positive modality.

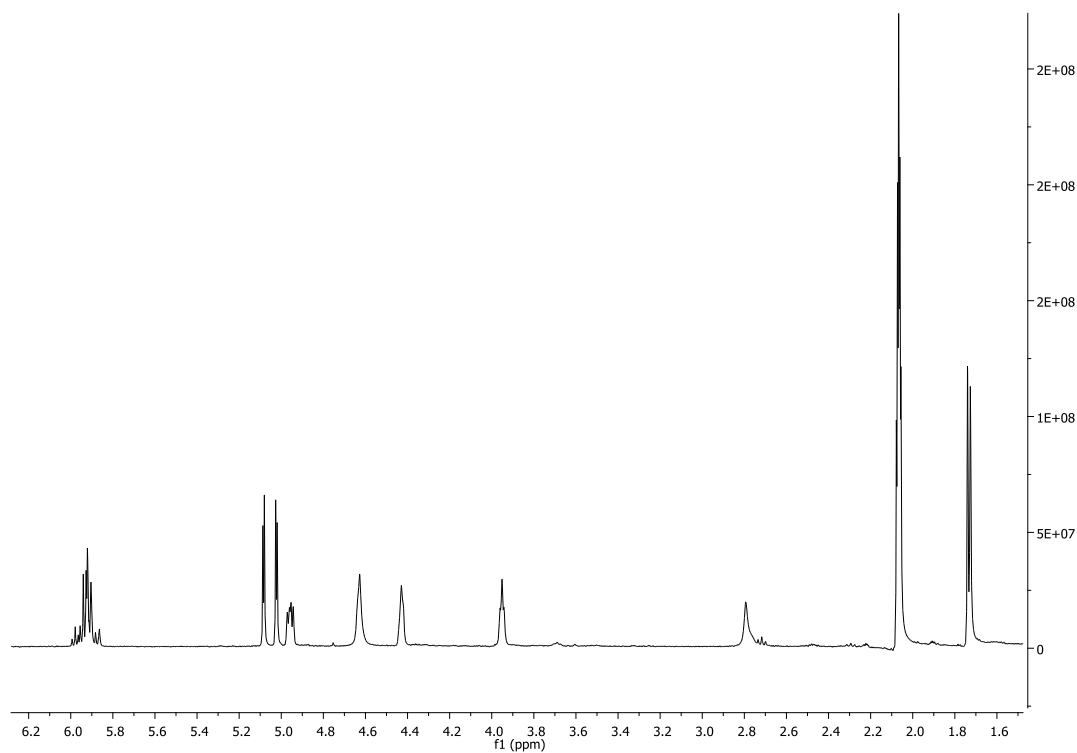


Figure S8. ^1H NMR of massarilactone H (**2**) recorded in acetone- d_6 at 500 MHz.

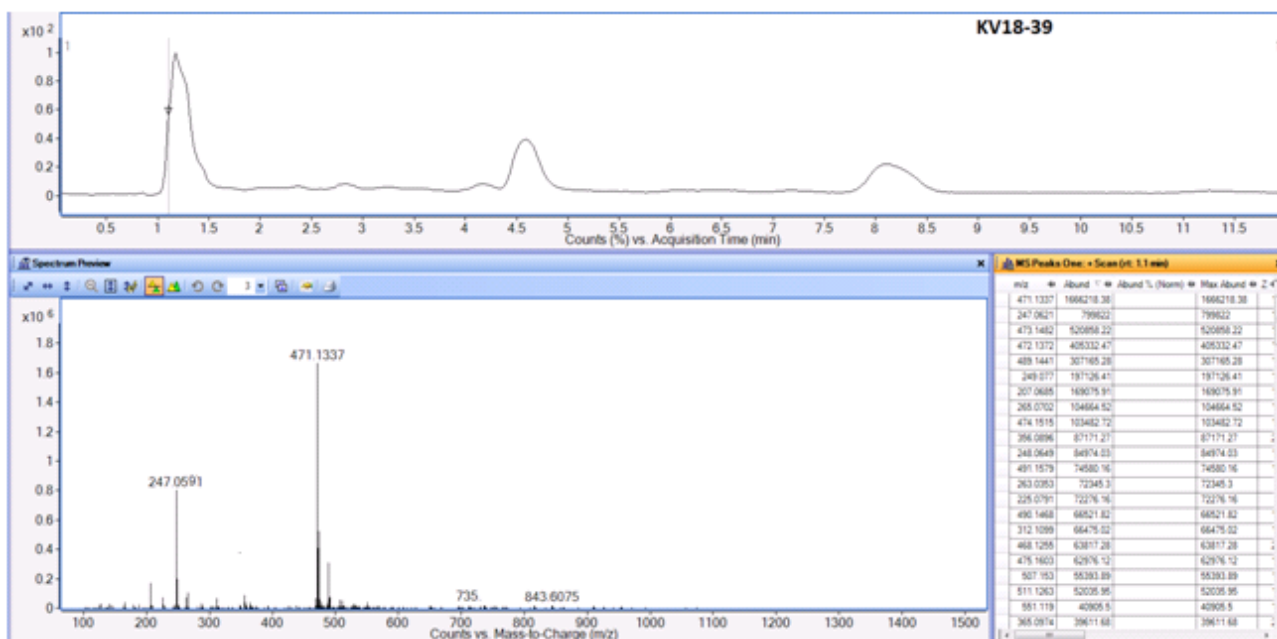


Figure S9. HR ESI MS of of massarilactone H (**2**), recorded in positive modality.

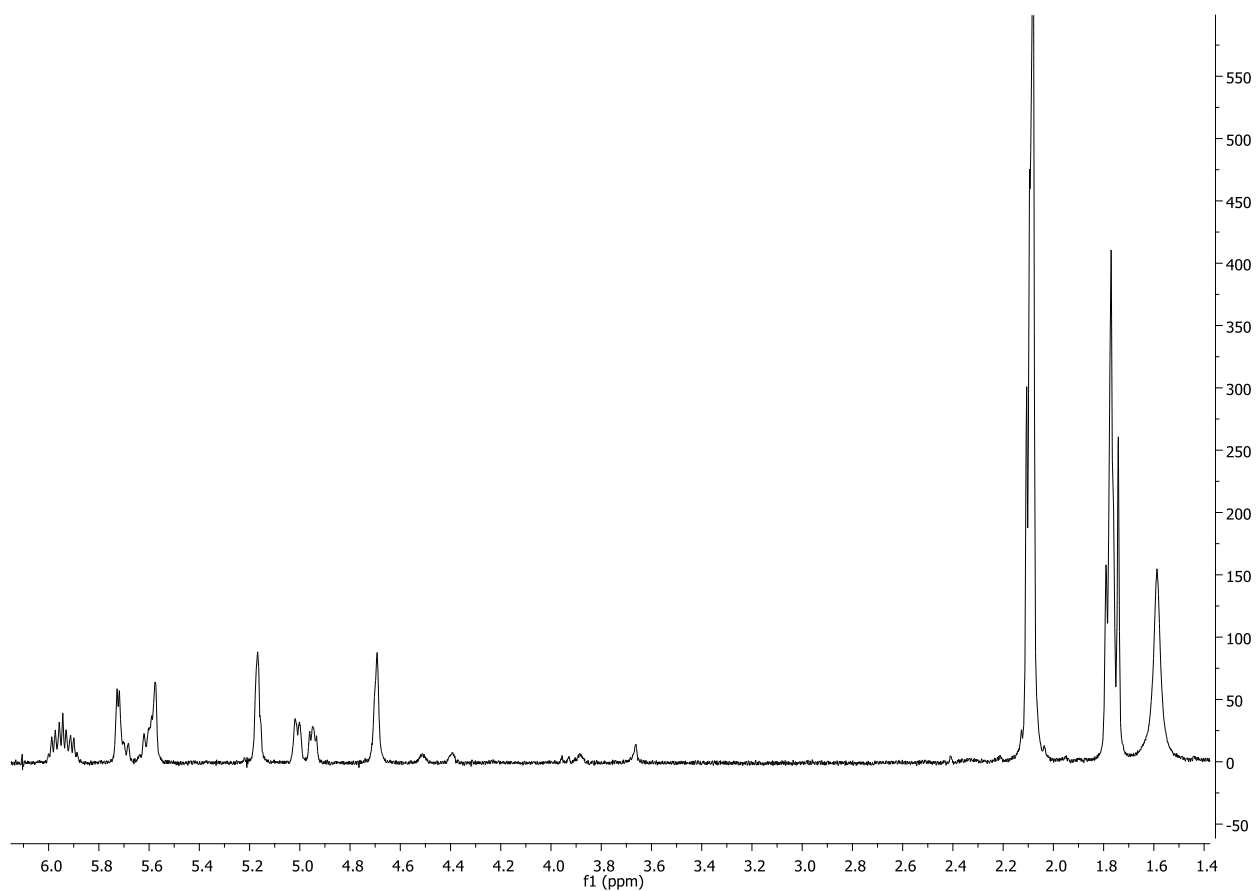


Figure S10. ^1H NMR of 3,4,7-*O',O'',O'''*-triacetyl derivative of massarilactone D (**3**) recorded in CDCl_3 at 500 MHz.

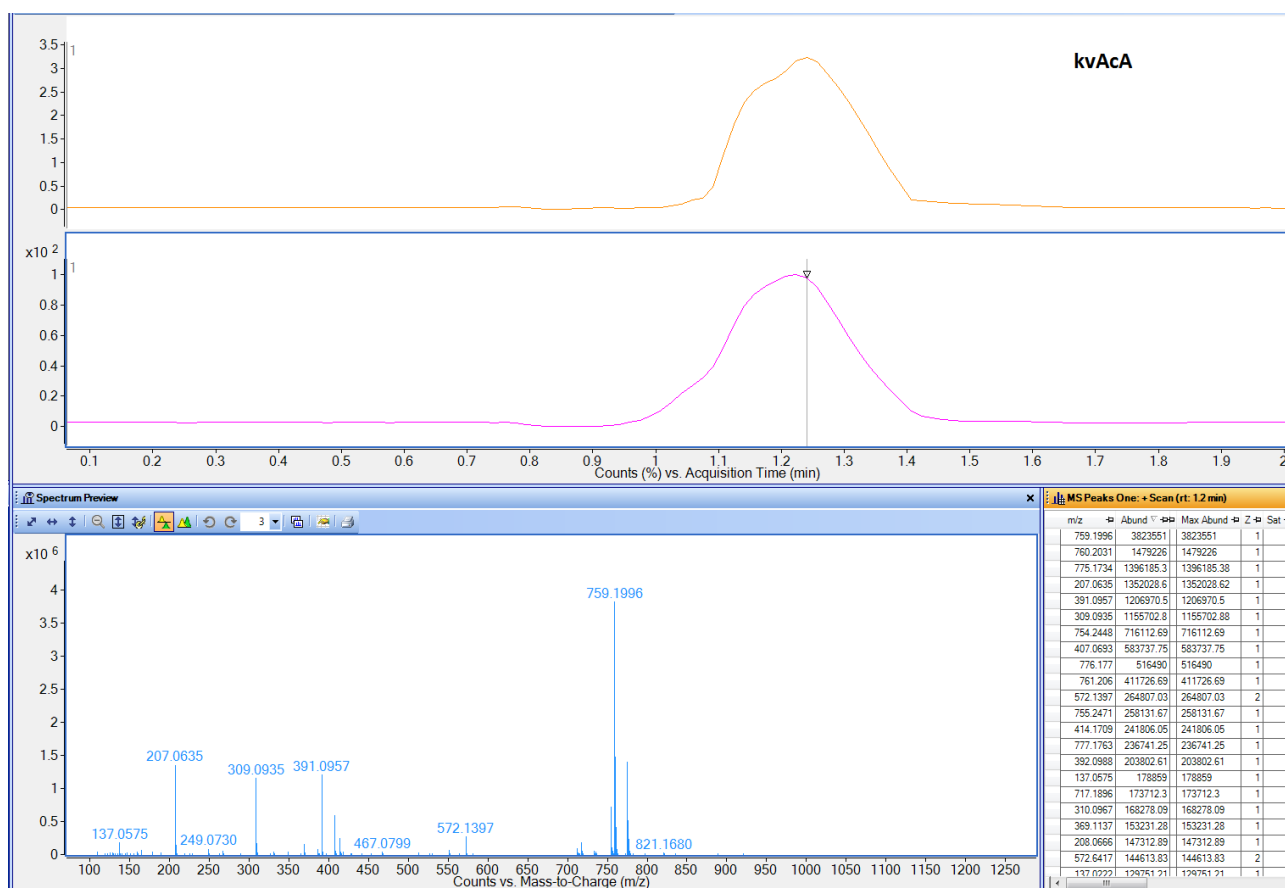


Figure S11. ESI MS of 3,4,7-*O,O',O''*-triacyl derivative of massarilactone D (**3**), recorded in positive modality.